Final Report

EXCITATION AND DEEXCITATION OF VIBRATION IN N_2 BY OXYGEN ATOMS

Prepared for:

ADVANCED RESEARCH PROJECTS AGENCY
WASHINGTON, D.C. 20301

U.S. ARMY RESEARCH OFFICE - DURHAM
BOX CM, DUKE STATION
DURHAM, NORTH CAROLINA 27706

CONTRACT DAHC04-70-C-0036
ARPA Order No. 1482
Program Code No. 62301 D

STANFORD RESEARCH INSTITUTE
Menlo Park, California 94025 · U.S.A.

71

STANFORD RESEARCH INSTITUTE
Menlo Park, California 94025 · U.S.A.

Final Report *October 1971*

EXCITATION AND DEEXCITATION OF VIBRATION IN N_2 BY OXYGEN ATOMS

By: GRAHAM BLACK and DONALD J. STROM

Prepared for:

ADVANCED RESEARCH PROJECTS AGENCY
WASHINGTON, D.C. 20301
Attention: MR. ROBERT MOORE

U.S. ARMY RESEARCH OFFICE - DURHAM
BOX CM, DUKE STATION
DURHAM, NORTH CAROLINA 27706
Attention: DR. ROBERT MACE

CONTRACT DAHC04-70-C-0036
ARPA Order No. 1482
Program Code No. 62301 D

SRI Project PYU-8626

Approved by:

FELIX T. SMITH, *Manager*
Molecular Physics Group

E. C. WOOD, *Director*
Applied Physics Laboratory

C. J. COOK, *Executive Director*
Physical Sciences Division

Copy No. 33

SYNOPSIS

The earth's upper atmosphere continuously emits infrared radiation. Some of this radiation is powered by the energy stored in vibrationally excited nitrogen, and it has been suggested that this is produced when nitrogen quenches $O(^1D)$. In this reaction the 1.96 eV electronic excitation of $O(^1D)$ is transferred to vibrational and rotational energy of the nitrogen and kinetic energy. Because no measurements of the fraction that appears as vibrational energy were available, the first task of the current program was to measure this fraction, using Raman spectroscopy to determine the population of $N_2(v=1)$ that is produced. During the course of the experimental program, a theoretical study by E. R. Fischer and E. Bauer concluded that less than 5% of the $O(^1D)$ electronic energy is channeled into the vibrational levels of N_2. Our experimental findings support their estimate. We obtain an efficiency of $8.3 \pm 6.5\%$ for the conversion of $O(^1D)$ electronic energy to N_2 vibrations. Further work with CO as an infrared tracer is desirable to confirm these findings and to increase the precision with which small vibrational populations can be measured.

Once produced, the vibrationally excited nitrogen is deexcited only by collisions. In the lower E-region (below 125 km) the major deexcitation process is by energy transfer to CO_2 with subsequent

emission. Above this height, the vibrationally excited nitrogen is removed by diffusion, by electron quenching, and by vibrational-translational energy exchange with $O(^3P)$. The reaction rate for the last process is not known for temperatures found in the earth's atmosphere. To measure it was the goal of the second task. The initial approach used laser-schlieren techniques to monitor post-shock relaxation processes in a shock tube. Boundary-layer disturbances were found to limit the usefulness of this technique, and it was abandoned in place of the infrared-tracer method first used by R. C. Millikan and D. R. White in 1963. Results are reported for N_2-1% CO, N_2-5% CO, and N_2-5% O_2-1% CO mixtures. Existing rate measurements suggest that the technique can be applied to N_2-O_2-O mixtures to obtain the required rate coefficients for vibrational-translational energy exchange of $N_2(v=1)$ with $O(^3P)$ down to $\sim 1400^{\circ}K$.

CONTENTS

FIGURES

FIGURES (continued)

TABLES

INTRODUCTION

Three years ago[1] it was suggested that vibrationally excited nitrogen is an electron heat source in the E-region and that the vibrational temperature of nitrogen is much greater than the neutral gas temperature. In addition to heating the electrons, the vibrationally excited nitrogen [N_2(vib)] can also transfer its energy to heteronuclear molecules (particularly CO_2) that radiate in the infrared. Processes that excite or deexcite N_2(vib) are thus of particular interest in connection with some defense problems concerned with atmospheric infrared measurements.

The main processes that have been considered for producing N_2(vib) are:

$$O(^1D) + N_2 \rightarrow N_2\ (v \leq 7) + O(^3P) \qquad (1)$$

$$N + NO \rightarrow N_2\ (v \leq 12) + O(^3P) \qquad (2)$$

$$e^- + N_2 \rightarrow N_2^- \rightarrow N_2\ (\text{vib}) + e^-. \qquad (3)$$

Whereas the third process is certainly important in auroral conditions, it is not important in the undisturbed E-region. Process (2) may yield[2-4] one third of the exothermicity in vibrational excitation although this result has been questioned by Wray.[5] Recent work[6] at Air Force Cambridge Research Lab suggests an even higher efficiency for converting the heat available in reaction (2) into vibrational energy.

Walker[1] assumed that process (1) was the most important source of vibrational excitation in nitrogen, the $O(^1D)$ being produced by photodissociation of O_2 in the Schumann-Runge continuum (the major energy input into the E-region of the atmosphere). Although subsequent theoretical estimates[7] suggest that this is not correct and that process (1) is inefficient in producing vibrational excitation, no experimental measurements had been made. Task I of this program was to make measurements using Raman spectroscopy to measure the vibrational state populations.

The most important deexcitation mechanisms for N_2 (vib) are

$$N_2\ (v=1) + CO_2 \rightarrow CO_2\ (\nu_3 = 1) + N_2, \qquad (4)$$

which has a large cross section ($\sim 10^{-3}$ gas kinetic) and dominates the other losses below 125 km (the $CO_2(\nu_3)$ then radiates). Above this altitude, N_2 (vib) is lost by diffusion, by electron quenching, and by

$$N_2\ (vib) + O \rightarrow N_2 + O, \qquad (5)$$

which is much faster than most vibration-translation processes of N_2 (vib) with species other than atomic oxygen.[8] The rate of process (5) in the E-region can be estimated by a long extrapolation of the data of Breshears and Bird[8] obtained at temperatures in the 3000 to 4500°K range. To reduce the uncertainty introduced by the long extrapolation, Task II of our program was to extend their measurements down to as low a temperature as possible.

TASK I. VIBRATIONAL POPULATION MEASUREMENTS

Background

The reaction

$$N_2\ (v=0) + O(^1D) \rightarrow N_2\ (v=n) + O(^3P) + \Delta E, \qquad (1)$$

where ΔE is the energy in rotational and translational modes, has been studied at room temperature in this laboratory[9] as well as in others.[10-17] A rate coefficient for quenching $O(^1D)$ of approximately 5×10^{-11} cm^3 $molecule^{-1}$ sec^{-1} was deduced from our experiments.[9] This rate coefficient not only agrees with the most recent measurements[15] but is in excellent agreement with the value deduced from dayglow observations.[18]

None of the experiments has provided any information on the fraction of the ^1D excitation energy (1.96 eV) that is converted into vibrational energy of the nitrogen molecule by the quenching reaction. Energetically, the quenching reaction (1) may produce nitrogen in any level up to n=7. It is expected[2,3,19-24] that the initial vibrational distribution will be rapidly degraded by vibrational exchange collisions of the type

$$N_2\ (v=n) + N_2\ (v=0) \rightarrow N_2(v=n') + N_2\ (v=n-n') \qquad (6)$$

or, effectively

$$N_2\ (v=n) + (n-1)\ N_2(v=0) \rightarrow n\ N_2\ (v=1) \qquad (6')$$

to produce a non-equilibrium population of N_2 (v=1). Hence, although our initial plan was to measure the concentration of N_2 (v=n) as a function of time for each value of $n \leqslant 7$ and thus deduce separate rate coefficients for each value of v=n in reaction (1), the rapid rate of reaction (6) makes this impossible. Measurement of N_2 (v=1) is, however, sufficient to determine the fraction of ^1D excitation energy that appears as vibrational energy (since the higher levels are in Boltzmann equilibrium with v=1). The measurements were made by observing Raman scattering of 4880-Å Ar^+ laser radiation. The intensity of the anti-Stokes transition at 4382 Å was measured because this is free from transitions due to the N_2 (v=0) level [whereas the Stokes transition from N_2 (v=1) at 5497 Å lies in the rotational structure of the Stokes line from N_2 (v=0) centered at 5506 Å].

The $O(^1D)$ atoms in the experiment are produced by photodissociation of O_2, using a Xe resonance lamp (1470 Å), in the reaction $h\nu$ (1470 Å) + $O_2 \rightarrow O(^1D) + O(^3P) + 1.4$ eV. The atoms are thus each produced with 0.7 eV translational energy (equivalent to $\sim$ 8000°K). We could, in principle, by adding an inert buffering gas in varying amounts, study reaction (1) over a range of energies, or equivalent temperatures.

Removal of N_2 (v=1) was by gas flow from the cell, deactivation on the cell walls, quenching by impurities, or by

$$N_2\ (v=1) + O_2\ (v=0) \rightarrow N_2\ (v=0) + O_2\ (v=1) \qquad (7)$$

or

$$N_2\ (v=1) + O(^3P) \rightarrow N_2\ (v=0) + O(^3P). \qquad (5)$$

We had hoped to obtain information on these rates by pulsing the Xe resonance lamp and observing the decay of the signal from $N_2(v=1)$. However, the very low signal strength (see Discussion) has precluded such measurements.

Experimental

The vibrationally excited nitrogen was produced by photolysis of a mixture of oxygen and nitrogen at 1470 Å. In all cases the mixture used con ained 0.25 Torr of oxygen (to provide an optical density of 1 for a path length of 10 cm and absorb essentially all the 1470 Å light) and a sufficiently higher pressure of nitrogen so that the major loss of $O(^1D)$ was by reaction (1) and not by

$$O(^1D) + O_2 \rightarrow O_2(b^1\Sigma_g^+) + O(^3P). \qquad (8)$$

A nitrogen pressure of 2 Torr was used in all experiments. At this pressure, over 90% of the $O(^1D)$ undergoes reaction (1) rather than reaction (8).[9] The concentration of the vibrationally excited nitrogen produced was determined by measuring the intensity of Raman scattering from a focused beam of 4880-Å Ar^+ laser radiation. The factor

for converting the intensity of Raman scattering from $N_2(v=1)$ to a concentration was determined by measuring the intensity for known pressures of N_2 (v=1) in heated air.

The experimental arrangement is shown in Figure 1. It consists of several major components. The nucleus of the experiment is the cell in which the oxygen-nitrogen mixture is irradiated with 1470-Å light. The output of an Ar^+ ion laser traverses this cell and is focused to a point within the cell. This focal point is then imaged on the slit of a spectrometer by a second optical system. The light passing through the exit slit of this spectrometer is imaged on the photocathode of a photomultiplier. Its output is measured in a pulse-counting system and then printed out after a predetermined counting time (governed by the setting of the controller).

The spectrometer is a Spex Model 1402 double spectrometer with a thermoelectrically cooled housing for the photomultiplier tube. A Fluke high voltage power supply (Model 412B) provides the photomultiplier voltage. The photomultiplier output is amplified and discriminated by an SSR Model 1120 photon counter before being fed to an Ortec gate and delay generator (Model 416A). The stretched output of this unit is then coupled to a Canberra Model 1480 linear ratemeter for counting and display on a pen recorder (Varian G-11 A). The stretched output of the Ortec Model 416A is compatible with the input of a Hewlett Packard

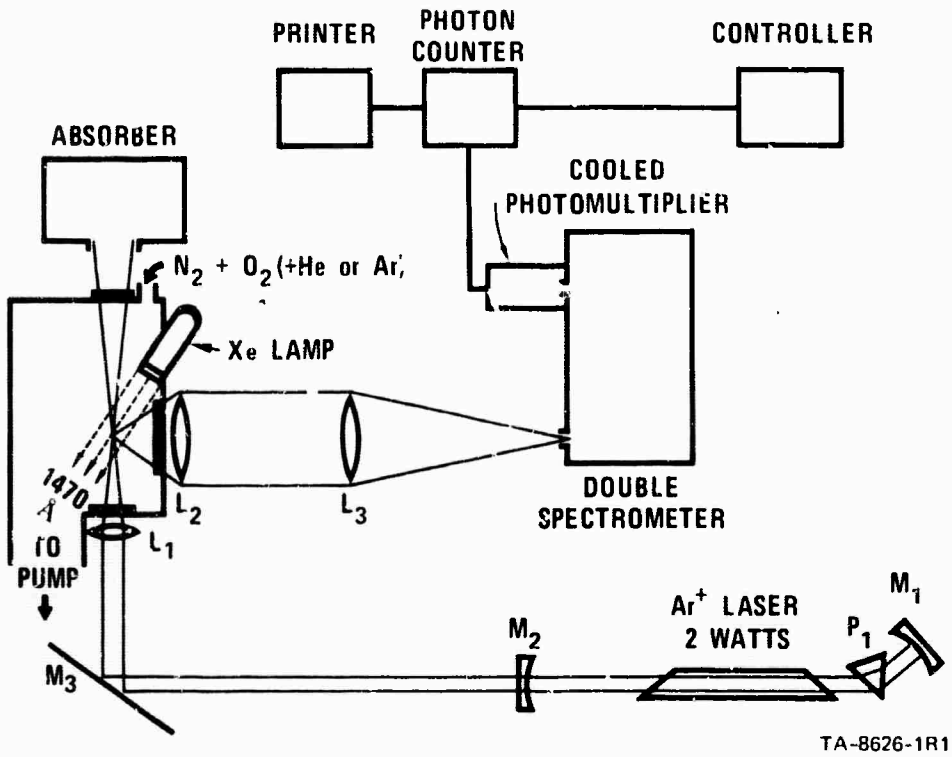

FIGURE 1 EXPERIMENTAL ARRANGEMENT FOR RAMAN SPECTROSCOPY. The lens L_2, which has an aperture ratio of f/0.95 and a focal length of 5.0 cm, collects the Raman-scattered light over a large solid angle

Model 523B Electronic Counter, which counts for a preset time (determined by the controller settings) before its final count is printed on an Hewlett Packard Digital Recorder Model 560A. The controller then initiates another counting sequence. The controller, which makes data-taking fully automatic, is constructed from Digital Equipment Modules.

The laser is an argon-ion laser (Coherent Radiation Laboratories Model 52A) equipped for single wavelength selection and providing 700 mW CW at 4880 Å. Mirror M_3 reflects the laser beam through 90° so that the Raman light can be focused on (not across) the spectrometer slit. To enhance the power density of the laser radiation, an antireflection-coated lens L_1 of focal length 3 in. converges the beam to a focus in the region that is the image of the spectrometer slit as formed by lenses L_2 and L_3. The lens L_2 is an f/0.95 Angenieux with a focal length of 5.0 cm. The lens L_3, an f/5.6 Carl Meyer Tele lens with a focal length of 16 in., was chosen to fill the acceptance cone of the spectrometer. Lenses L_1 and L_2 are mounted in positioners (Gaertner Scientific No. R287) allowing motion in three mutually perpendicular directions. The absorber is the absorption head of a Coherent Radiation Model 201 Broad Band CW Laser power meter, which is connected to a meter readout that monitors the laser power. All the optical components (with the exception of the laser) are mounted on an optical bench

attached to the front of the spectrometer. All the equipment is on a vibration-free concrete table.

The microwave-powered Xe resonance lamp (Figure 1) is a standard item of equipment in this laboratory and has been in use for several years.[9,25,26] It incorporates a sapphire window connected to the lamp body through a graded seal, is filled with Xe at ~ 1 Torr and has a Ba-Al-Ni getter to maintain gas purity. It can be operated in either a continuous or pulsed mode with an intensity of $\sim 3 \times 10^{15}$ quanta/sec in the resonance line. The visible emission from this lamp is particularly rich in blue light, which is the wavelength region in which we observe the anti-Stokes line of $N_2(v=1)$. In fact there is a XeI line at 4384 Å, only 2 Å away from the anti-Stokes line at 4382 Å. Hence the cell was designed with Wood's horns to minimize the scattering of light from the Xe lamp into the focusing optics for the spectrometer. The outside of the cell was sprayed with a flat black paint to further reduce scattered light. With these precautions the scattered light from the photolysis lamp gave ~ 0.3 counts/sec with the spectrometer set at the 4382 Å anti-Stokes line of N_2 (v=1). There was also a small scattered light signal from the 4880-Å laser beam (with the spectrometer set at 4382 Å), but this was about an order of magnitude smaller.

Several different photomultipliers were tried during the course of this work. The principal ones were an FW 130 with a 0.1-inch diameter photocathode, an FW 130 with a 0.35-inch photocathode, and an EMI 6256S with a 10-mm photocathode. Twenty dB of attenuation (from an Hewlett Packard 355D VHF Attenuator) was inserted in the line between the photomultiplier base and the SSR photon counter to provide the greatest freedom from rf pickup. Despite this (and other) precautions, pickup from Tesla coil operation in adjacent laboratories gave very large counting rates. Such operation was therefore discouraged during our experimental runs. The system was also very efficient in detecting flickering fluorescent lights. These were either replaced or extinguished. In all cases the best signal-to-dark count was obtained at a voltage providing a 70% counting efficiency.

Before making any Raman measurements, the position of lenses L_1 and L_2 was adjusted to provide the biggest Rayleigh scattered light signal (with N_2 at atmospheric pressure in the cell) using the 4545-Å laser line (the shortest wavelength laser line and hence closest in wavelength to the position of the anti-Stokes line at 4382 Å). This focus was periodically checked but found to require very little adjustment on a daily basis. The spectrometer was normally used with an entrance slit width of 250 μ (giving a bandwidth of 1.3 Å) and a length of 10 mm with intermediate and final slits of 500μ. The wavelength error in the read-

out of the spectrometer was periodically checked with the Hg 4358 Å line. It did not change during the course of these measurements.

Measurements of the anti-Stokes line at 4382 Å in heated nitrogen established that the larger photocathode FW 130 and the EMI 6256S had the same sensitivity, whereas the 0.1-inch diameter photocathode FW 130 had a sensitivity down by a factor of 2.4 (see Results). To compensate for this factor and make it easier to combine measurements with all three photomultipliers, we used a counting time of 12 minutes with the last tube and 5 minutes with the first two tubes.

Because of the scattered light from both the microwave lamp and the laser, the Raman signal had to be extracted from the counts, C_i, obtained in four consecutive counting periods of equal length. From such a sequence which we define as an "experiment," the Raman signal arising from the $O(^1D) - N_2$ interaction is obtained from

$$\text{Raman counts} = C_2 + C_4 - C_1 - C_3 , \qquad (9)$$

where C_2 is the count obtained with both microwave lamp and laser on (and hence includes the Raman signal together with the scattered light from both sources and the dark count), C_4 is the photomultiplier dark count (both light sources off), C_1 is the count with only the laser on, and C_3 is the count with only the microwave lamp on. This operation also subtracts from the Raman count the signal arising from Raman scattering of the laser radiation by the small (2.8×10^{-5} Torr) population of $N_2(v=1)$ which is present in 2 Torr of nitrogen at 27°C.

Three gas mixtures were investigated. These were 0.25 Torr oxygen and 2 Torr nitrogen without any buffer gas and with helium (10 Torr) or argon (20 Torr) as buffer gases. The addition of buffer gas had two functions: to thermalize the translationally hot $O(^1D)$ and $O(^3P)$ and also to reduce the rate of $N_2(v=1)$ diffusion to the walls. However, the amount of helium that can be added to achieve these effects is limited because it can also convert the vibrational energy of $N_2(v=1)$ into kinetic energy. The efficiency of this process can be estimated from the expression[27]

$$\log_{10}(p\tau_v) = 5.0 \times 10^{-4} \mu^{\frac{1}{2}} \theta^{4/3} \left(T^{-1/2} - 0.015\mu^{1/4}\right) - 8.0, \quad (10)$$

where τ_v(sec) is the lifetime of the relaxing species with vibrational quantum temperature $\theta(^oK)$ against quenching in collisions with a species at pressure p (atm). The reduced mass of the colliding particles is μ (atomic mass units) and $T(^oK)$ is the kinetic temperature. At 300°K, this expression yields

$$(p\tau)_{N_2\text{-He}} = 1.8 \times 10^{-2} \text{ atm sec.} \quad (11)$$

Hence the helium cannot be used at pressures much greater than 10 Torr without itself causing a significant loss of $N_2(v=1)$, and thereby reducing the sensitivity of the measurements. For argon at 300°K, Equation (10) yields

$$(p\tau)_{N_2\text{-Ar}} = 3.3 \times 10^4 \text{ atm sec.} \quad (12)$$

Hence argon is $\sim 10^{-6}$ as efficient as helium, and much higher pressures can be used without quenching $N_2(v=1)$.

Results

Table I presents the actual counts obtained in a series of experiments comprising a typical run, on one of the gas mixtures used. In this case, each count was taken over a period of 300 seconds. In practice, a "run" lasted until one of the experimental parameters (i.e., gas mixture, phototube, pumping speed) was changed or a malfunction in one of the system components occurred. All the experiments comprising a single run were averaged and statistically analyzed. Some experiments were then rejected because one of the counts C_i was unacceptably too large or too small (almost always too large). The rejection criterion adopted was Chauvenet's criterion[28] which was applied not only to the individual counts obtained in a sequence of experiments but to the Raman counts (final column of Table I) as well. For the sequence of experiments shown in Table I, the acceptable spread of results is shown in the final line of the table. All the data fall within these limits. Applying Chauvenet's criterion resulted in approximately 1% of the individual counts, and hence 5% of the experiments, being rejected. In most of the rejected cases, a much too large count rate was observed which could frequently be correlated with a spurious noise pulse in the output of the photon counting system (shown as a spike on the pen recorder trace of the output of the ratemeter).

In 4 months of taking the final data, approximately 770 experiments

TABLE I

DETERMINATION OF RAMAN SIGNAL

O_2 = 0.25 Torr, N_2 = 2 Torr, photon counts in 5-minute periods using an EMI 6256S at 1145 V (70% counting efficiency).

Experiment	C_1 Counts	C_2 Counts	C_3 Counts	C_4 Counts	Raman Signal = $C_2+C_4 - C_1 - C_3$ Counts
1	2048	2171	1821	1765	67
2	2148	2040	1813	1776	-145
3	2042	2123	1893	1773	-39
4	2161	2047	1815	1774	-155
5	2089	2134	1783	1877	139
6	2083	2209	1707	1779	198
7	2020	2099	1863	1822	38
8	2027	2187	1875	1814	99
9	2056	2259	1803	1805	205
10	2113	2143	1861	1798	-33
11	2188	2121	1835	1764	-138
12	2051	2196	1857	1773	61
13	2117	2223	1838	1827	95
14	2134	2158	1803	1809	30
15	2058	2221	1827	1857	193
16	2062	2077	1810	1844	49
17	2134	2144	1814	1874	70
18	2044	2084	1806	1779	13
19	2204	2141	1800	1862	-1
20	2139	2123	1815	1816	-15
21	2170	2179	1827	1862	44
22	2192	2165	1803	1763	-67
23	2178	2091	1776	1841	-22
24	2151	2134	1841	1712	-146
25	2141	2108	1795	1812	-16
26	2075	2117	1803	1755	-6
27	2061	2094	1740	1820	113
28	2140	2p38	1899	1787	-114
29	2142	2058	1903	1759	-228
30	2141	2222	1909	1786	-42
31	2178	2016	1803	1821	-144
32	2195	2177	1947	1905	-60
33	2147	2213	1720	1758	104
34	2137	2158	1793	1790	18
35	2136	2046	1827	1805	-112
Mean =	2117.20	2137.60	1823.57	1804.69	1.51
σ =	53.77	59.45	50.65	42.06	108.13
$2.45 \times \sigma$ =	132	146	124	103	285

were completed and, of these, 732 were acceptable. Most of these (355) were made with the argon buffer gas, 207 were made with the helium buffer gas, and 170 were made with no buffer gas. For each of the three gas mixtures, in addition to evaluating $\bar{x}$ (counts/sec), the mean Raman counting rate, we also calculated the estimated error of the mean, $p_{\bar{x}}$, from

$$p_{\bar{x}} = \frac{\sigma_x}{\sqrt{N}} \qquad (13)$$

where σ_x is the standard deviation of the individual x values and N is the number of such values. This was computed for each of the three sets of experiments at intervals of twenty experiments. From a normal distribution of similarly determined means, only 32% should deviate from the grand mean by an amount greater than $p_{\bar{x}}$ and less than 5% should deviate by more than $2p_{\bar{x}}$. The values of $\bar{x}$ with error limits calculated from equation (13) are shown in Figures 2, 3 and 4 for the gas mixtures as a function of the number of measurements, compiled as the data were taken. Note that these figures simply show the historical trend of the results as the data were accumulated; the final result for each gas mixture is given by the accumulated results of all the experiments (farthest point to the right on the abscissa).

To convert the measured Raman counts/sec into a partial pressure of $N_2(v=1)$, we measured the intensity of the anti-Stokes line at 4382 Å with nitrogen alone in the cell. As Table II shows, the pressure of $N_2(v=1)$ in air provides a very convenient means of determining the sensitivity of our apparatus for this species.

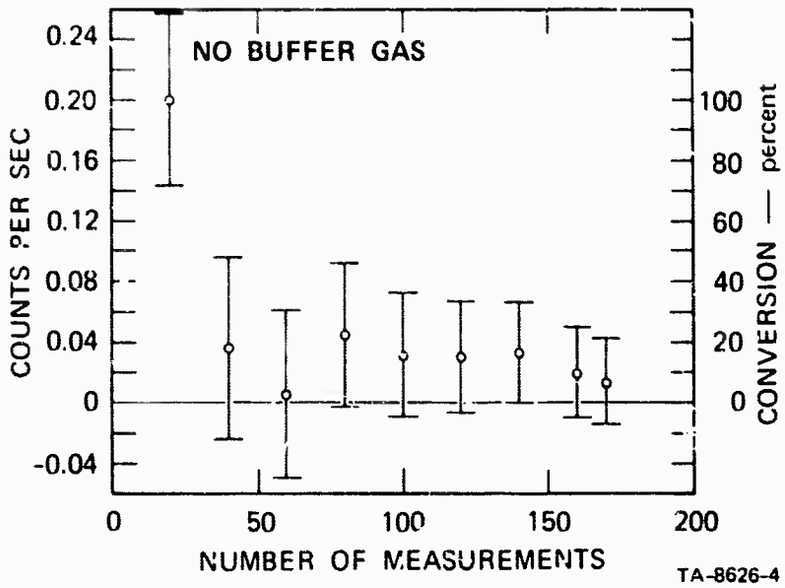

FIGURE 2 RAMAN SIGNAL AT 4382 Å [Anti-Stokes Line of $N_2(v = 1)$ For Scattering Ar^+ Laser Emission at 4880 Å] FROM A MIXTURE OF N_2 = 2 TORR AND O_2 = 0.25 TORR UNDERGOING 1470 Å IRRADIATION

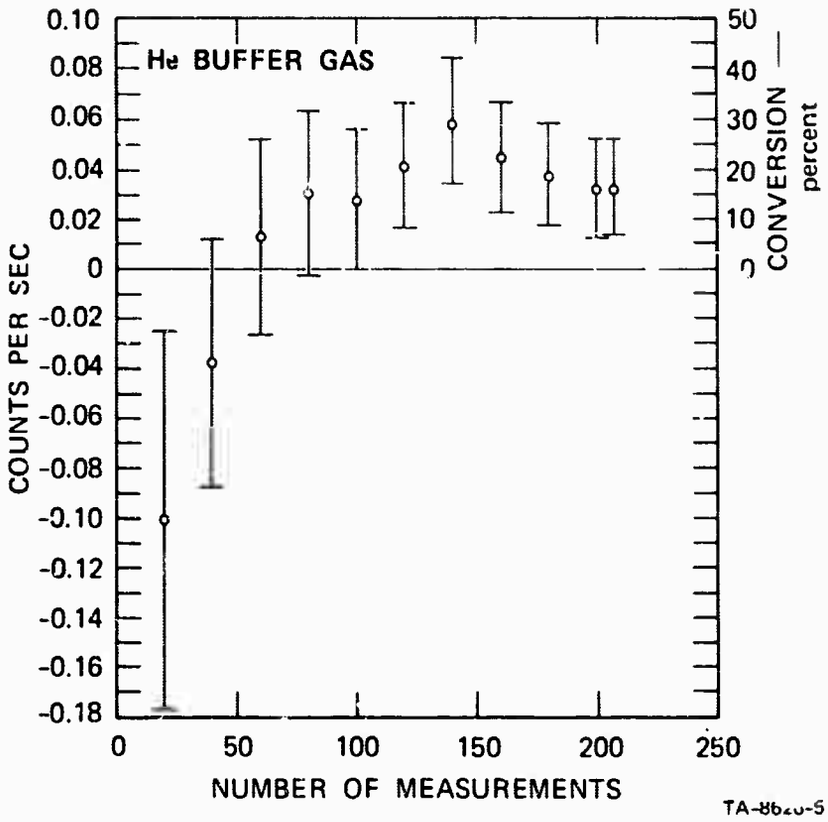

FIGURE 3 RAMAN SIGNAL AT 4382 Å [Anti-Stokes Line of $N_2(v = 1)$ For Scattering Ar^+ Laser Emission at 4880 Å] FROM A MIXTURE OF He = 10 TORR, N_2 = 2 TORR, AND O_2 = 0.25 TORR UNDERGOING 1470 Å IRRADIATION

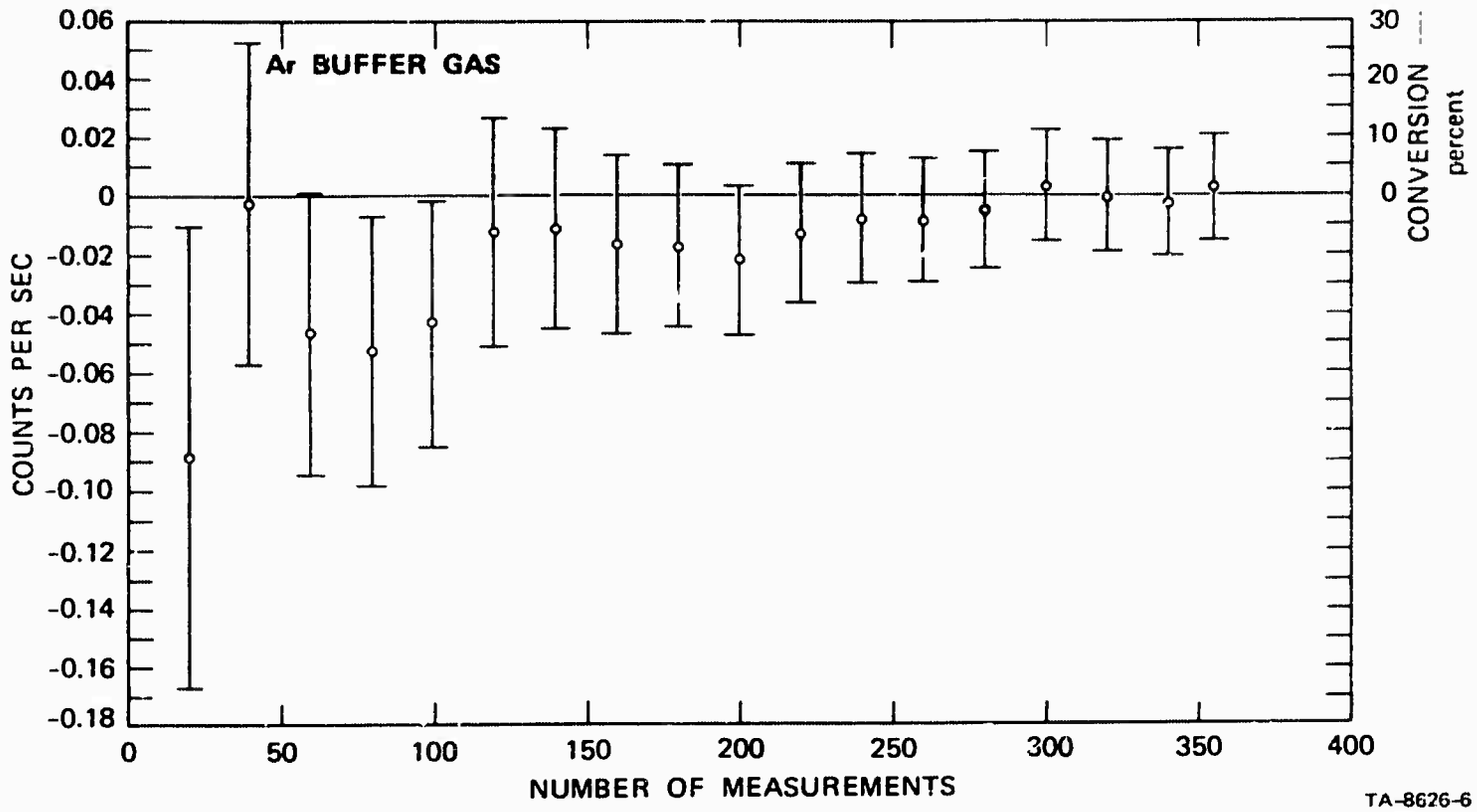

FIGURE 4 RAMAN SIGNAL AT 4382 Å [Anti-Stokes Line of $N_2(v = 1)$ For Scattering Ar^+ Laser Emission at 4880 Å] FROM A MIXTURE OF Ar = 20 TORR, N_2 = 2 TORR, AND O_2 = 0.25 TORR UNDERGOING 1470 Å IRRADIATION

TABLE II

PRESSURE OF $N_2(v=1)$ IN AIR AT VARIOUS TEMPERATURES

Temperature, °C	$[N_2(v=1)]/[N_2(v=0)]$	$[N_2(v=1)]$ Torr in Air at 760 Torr
-50	2.96×10^{-7}	1.76×10^{-4}
-30	1.02×10^{-6}	6.05×10^{-4}
-10	2.91×10^{-6}	1.73×10^{-3}
5	5.79×10^{-6}	3.44×10^{-3}
27	1.40×10^{-5}	8.31×10^{-3}
50	3.11×10^{-5}	1.85×10^{-2}

These measurements established that with the EMI 6256S and the larger photocathode FW 130, the apparatus had a sensitivity of 300 counts sec^{-1} $[Torr\ N_2(v=1)]^{-1}$, whereas with the FW 130 with the 0.1-inch diameter photocathode the sensitivity was 125 counts $sec^{-1}[Torr\ N_2(v=1)]^{-1}$. In an earlier report,[29] we had calculated that 100% conversion of the $O(^1D)$ energy to excitation of $N_2(v=1)$ would yield $[N_2(v=1)] = 6.6 \times 10^{-4}$ Torr. Hence 100% conversion would correspond to a signal of 0.20 counts/sec with the most sensitive photomultipliers. It is on this basis that the percent conversion scale was drawn on the right hand sides of Figures 2, 3 and 4.

Combining the data from the He and Ar buffer gas mixtures, we obtain an efficiency of 8.3 ± 6.5% for the conversion of $O(^1D)$ electronic energy to N_2 vibrations (see Discussion).

Discussion

We shall first mention the results for the unbuffered N_2(2 Torr) - O_2(0.25 Torr) mixture, which yielded a value of 7 ± 14% for the energy conversion efficiency. In this mixture the hot (0.7 eV) $O(^3P)$ and $O(^1D)$ atoms produced in the O_2 photolysis can react with N_2 before they are thermalized. Thus, in addition to the fact that the quenching reaction

$$O(^1D) + N_2 \rightarrow O(^3P) + N_2(v \leq 7) \qquad (1)$$

can occur at high translational energies, we also find that N_2(vib) can be excited by translational-vibrational processes, e.g.

$$O + N_2 \rightarrow O + N_2(v=1), \qquad (14)$$

Here either the ^1D or ^3P state of O may take part, but it is unchanged by the collision.

The efficiency of (14) (at least for $O(^3P)$) can be estimated from the data of Breshears and Bird.[8] We have fitted their data for the vibrational relaxation time τ(μsec) of nitrogen by oxygen atoms at pressure p (atm) with the expression

$$\log [p\tau] = -3.66 + 54.5\ T^{-1/3}, \qquad (15)$$

where T is the temperature in °K.

To convert the relaxation time τ into a probability for vibrational relaxation, P_{10}, we solved the expression

$$\tau = [P_{10}Z(1 - e^{-hc\omega/kT})]^{-1}, \qquad (16)$$

where Z is the collision frequency and ω is the vibrational spacing in cm^{-1}. We then calculated the probability for vibrational excitation of nitrogen by oxygen atoms (P_{01}) from the expression

$$P_{01} = P_{10}\, e^{-hc\omega/kT}. \qquad (17)$$

This probability is shown as a function of temperature in Figure 5. It can be seen that at the temperature corresponding to 0.7 eV (8100°K) this probability is only 0.02. If the efficiency is similar for converting the translational energy of the $O(^1D)$ atoms produced in the O_2 photolysis, then process (14) represents (including both atoms) a small source of $N_2(v=1)$ in the unbuffered N_2 - O_2 mixture, equivalent to the 0.5% conversion efficiency for $O(^1D)$. This result is consistent with the lack of a substantial signal in those experiments (Fig. 2) when compared to the buffered cases, but the experimental uncertainties preclude a good estimate of the efficiency of process (14).

The thermalizing effect of He and Ar in the other two gas mixtures studied is sufficient to leave reaction (1) as the only possible significant source of $N_2(v=1)$. The Ar-buffered mixture yielded a value of 1.0 ± 8.9% for the conversion efficiency, and He-buffered mixture gases 16.4 ± 9.4%. One should be reminded that these values are based on an estimate of 1 sec for the effective lifetime of $N_2(v=1)$ in the system.

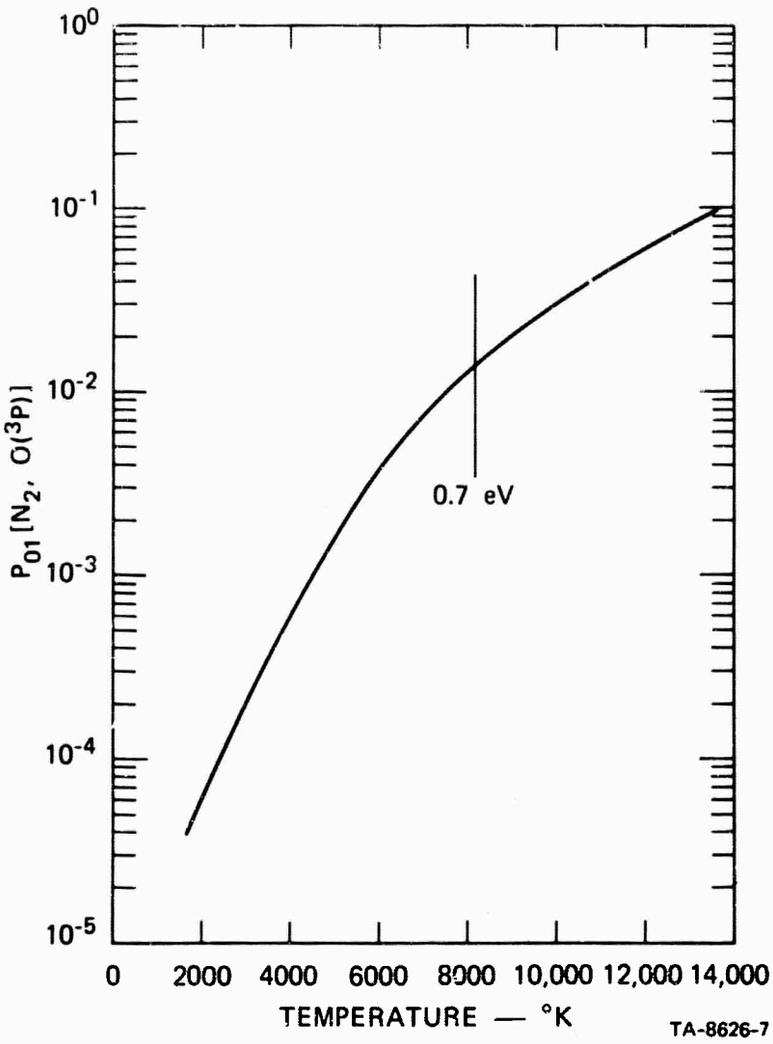

FIGURE 5 PROBABILITY OF EXCITING $N_2(v = 0)$ TO $N_2(v = 1)$ BY COLLISIONS WITH $O(^3P)$ VERSUS TEMPERATURE

The steady-state density of $N_2(v=1)$ is proportional to this lifetime, thus the derived conversion efficiency is proportional to its inverse. In addition to their thermalizing action, the buffer gases tend to slow down diffusion to the wall. The Ar at 20 Torr will be more effective in this role than the He at 10 Torr, and if spatial diffusion were limiting the $N_2(v=1)$ loss, more Raman signal should be seen with Ar as a buffer than with He. This consideration, and the fact that the statistical error bars overlap leads to the conclusion that the larger signal observed with He is statistically insignificant, and the two results are compatible. In fact, both diffusion times are estimated to be $\leq 10^{-1}$ sec, thus the lifetime is sustained by the slowness of wall interactions and the two buffer gas mixtures should yield the same results since both are sufficiently dense to thermalize the O atoms, as mentioned above. If wall reactions are faster or contaminants are present that reduce the lifetime, the $O(^1D)$ energy conversion efficiencies should be raised above the values we have calculated for the observed signals. The extreme weakness of the Raman signals have prevented an experimental measurement of the actual lifetime during the time of this contract, however such a measurement should be possible in follow-on work using CO as an infrared-active tracer gas.

Because the He and Ar results are felt to be compatible, we have combined them, weighted by the inverse square of the errors in the means

and find a value of 8.3 ± 6.5% for the conversion efficiency. The indicated error is again a standard deviation of the mean of the combined results; uncertainties in the effective $N_2(v=1)$ lifetime have not been included.

Summary

The results of the experiment lend support to a recent theoretical estimate[7] that the efficiency for converting the electronic energy of $O(^1D)$ into $N_2(vib)$ is as low as 2%. The technique we have used here is, however, clearly not sensitive enough to measure such a small value. It should further be cautioned that the experimental sensitivity is based on the assumption that the lifetime of $N_2(v=1)$ is governed by wall losses and is one second. A lifetime shorter than this (perhaps governed by impurity quenching) would raise the experimental values for the conversion figures given above. Clearly the measurement of the lifetime of $N_2(v=1)$ in the apparatus is required to put this study on a firm basis. It is for this reason that more sensitive measurements using CO as an infrared tracer gas have been suggested for the second year of the study.

TASK II. MEASUREMENT OF HIGH-TEMPERATURE VIBRATIONAL RELAXATION OF SHOCK-HEATED N_2 BY $O(^3P)$

Background

A number of experiments have recently been reported in which the vibrational relaxation of a diatomic gas by chemically active atomic species was studied. These include the effects of $O(^3P)$ on O_2 by Kiefer and Lutz[30], of $O(^3P)$ on N_2 by Breshears and Bird,[8] of H on CO and of Fe on CO by von Rosenberg et al.[31, 32] In all cases, the relaxation times for diatom-atom collisions are considerably shorter than would be predicted from correlations based on reduced mass (e.g. Millikan and White[27]); furthermore, rotation-vibration energy transfer and resonant-vibrational energy transfer effects, which can produce rapid vibrational relaxation, are not present in these systems. For the $O-O_2$ and $O-N_2$ cases, and speculatively for the Fe-CO case, the rapid vibrational energy transfer has been attributed to a "chemical" effect, since in each case there is an attractive chemical bond. Other explanations may be possible, however. For example, Bauer and Tsang[33] predicted the high efficiency of the $O-O_2$ exchange on the basis of atom displacement reactions, although this is not applicable to the other systems. Alternatively, Parker[30] has fit the $O-O_2$ results of Kiefer and Lutz by using semiclassical collision theory with an angle-dependent Morse potential which has a strong repulsive part. Benson[30] feels

that the high efficiency of vibrational relaxation by atoms is due to the formation of metastable species. More recently, Bauer and Fisher have made calculations for the $O-N_2$ system using a curve-crossing model (see, e.g., Ref. 34). Although their results are not yet published, Bauer has indicated[35] that they predict the high efficiency with which O atoms relax N_2 at high temperatures, as measured experimentally by Breshears and Bird, but that the efficiency is expected to decrease markedly at lower temperatures ($\sim 1000^{o}K$).

Breshears and Bird measured the vibrational relaxation of N_2 by $O(^3P)$ atoms in the range $3000^{o}K < T < 4500^{o}K$. The objective of Task II of this project was to extend these measurements as far as possible to the lower temperatures found in the E-region of the earth's atmosphere ($\sim 1000^{o}K$).

We originally hoped that the laser-schlieren measurement technique that they used could be used also at the lower temperatures. However, as described below, the method becomes limited by disturbances from boundary-layer turbulence at approximately $3000^{o}K$, and after considerable effort was expended to surmount the problems we concluded that an alternate measurement technique was required. The only technique that has been successfully applied to the measurement of the vibrational relaxation of N_2 at temperatures well below $3000^{o}K$ is the infrared-tracer method first used by Millikan and White[36]. In

this technique, a small amount (typically 1%) of CO is added to the test gas. The infrared radiation from the CO is then taken as proportional to the vibrational energy of the N_2. This method has been adapted and developed for application to the present program, and a number of measurements have been completed that verify the performance of the shock tube, the measurement system, and the data analysis techniques.

In following sections of this report, we will discuss the design of the experiments, the theoretical basis of the IR-tracer method, and the experimental details. The laser-schlieren tests will then be described, followed by the IR measurements and results obtained to date. Finally, the extension of the IR technique to measurements involving atomic oxygen, and the limitations anticipated, will be described.

Experimental

Design of the Experiment

The unique feature of these experiments is the addition of ground-state atomic oxygen $O(^3P)$ to the primary N_2 gas. This can be accomplished by shocking a mixture of O_3 and N_2, with the O_3 dissociating to $O_2 + O$. In this section we discuss the chemical reactions that take place in the gas mixture and their rates. A comparison of these reaction rates with vibrational-relaxation rates for these gases and their mixtures is then made to examine whether the chemical reactions impose any limitations on the vibrational-relaxation measurements. The section concludes with a discussion of the effect of having O_2 present in the gas mixture.

The primary reactions of interest are[37]

$$M + O_3 \underset{k_{-18}}{\overset{k_{18}}{\rightleftarrows}} M + O_2 + O \tag{18}$$

$$O + O_3 \xrightarrow{k_{19}} O_2 + O_2 \tag{19}$$

and

$$O_2 + M \underset{k_{-20}}{\overset{k_{20}}{\rightleftarrows}} O + O + M, \tag{20}$$

where M is any particle (in this case, M is predominantly N_2). There is some disagreement concerning the pertinent rates; here, we will use the values chosen by Myers and Bartle[38] for reactions (18) and (19) and that of Wray[39] for reaction (20) (adjusted upward by a factor of 2 to account for the differences between N_2 and Ar catalysts):

$$k_{18} = 3.4 \times 10^{11}\ T^{\frac{1}{2}}(24{,}350/RT)^{1.75} \exp(-24{,}350/RT)\ \mathrm{cm^3\ mole^{-1}\ sec^{-1}}$$

$$k_{19} = 1.04 \times 10^{12}\ T^{\frac{1}{2}} \exp(-5{,}288/RT)\ \mathrm{cm^3\ mole^{-1}\ sec^{-1}}$$

and

$$k_{20} = 5.0 \times 10^{16}\ T^{-\frac{1}{2}} \exp(-118{,}000/RT)\ \mathrm{cm^3\ mole^{-1}\ sec^{-1}}:$$

At high temperatures, reaction (18) predominates over reaction (19) and can be assumed to proceed stoichiometrically. The O atoms formed then recombine on a much slower time scale by the reverse of reaction (20) until equilibrium is achieved. At still higher temperatures where a significant amount of O_2 is normally dissociated, both recombination and dissociation may be observed in a single test[39]. At the lower temperatures of interest in these experiments, reactions (18) and (19) both proceed competitively, so that there are fewer O

atoms than original O_3 molecules. Wray[39] has shown that the number of oxygen atoms formed behind the shock front is approximately related to the number of ozone molecules initially present $[O_3]_i$ by

$$[O] \cong [1 - \Psi_{O_3}(k_{19}/k_{18})] [O_3]_i , \qquad (21)$$

where Ψ_{O_3} is the mole fraction of ozone in the gas mixture. In view of the ratio of k_{19} to k_{18} given by the expressions above, and of the small value of Ψ_{O_3} (say, 0.01), it might be expected that reaction (19) will become important at temperatures below 2000°K.

To compare the time scale of these chemical reactions with vibrational relaxation times of interest, we converted the rate constants k_{18} and k_{20} to pseudo-dissociation times normalized to 1 atmosphere pressure. The results are presented in Figure 6, together with literature values[27] for the vibrational relaxation times for N_2, O_2, and CO, and for N_2-5%O_2[40] and N_2-3%O_3[8] mixtures. We see that the ozone dissociation is rapid compared with the relaxation times, while the O_2 dissociation is negligibly slow. Thus the completion of reactions (18) and (19) can be assumed as initial conditions of the vibrational relaxation.

Two other chemical reactions of possible importance in N_2-O_2-O mixtures are the recombination reverse of reaction (20) and an exchange reaction, namely

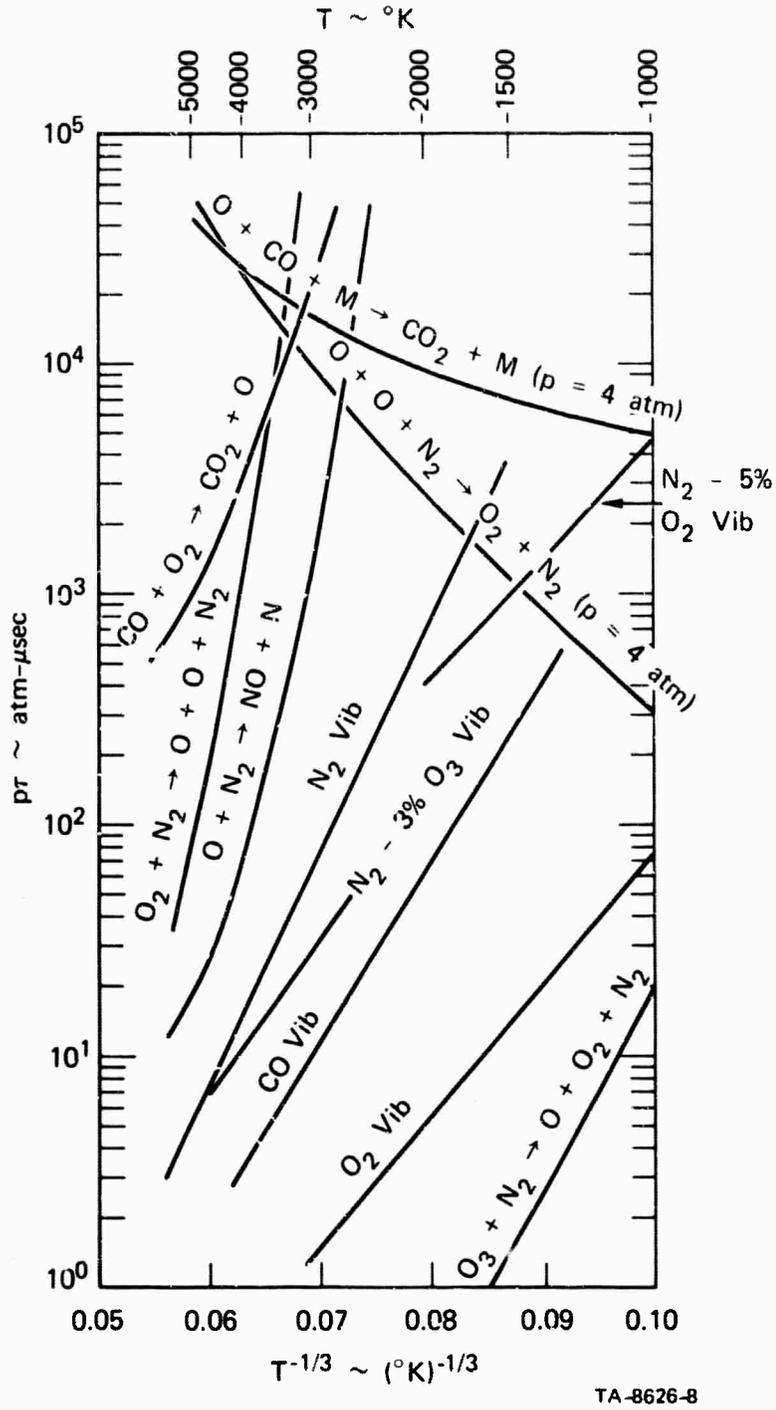

FIGURE 6 COMPARISON OF SELECTED VIBRATIONAL RELAXATION AND CHEMICAL REACTION TIMES FOR N_2-O_2-O-CO MIXTURES

$$O + O + M \rightleftharpoons O_2 + M \qquad (-20)$$

and

$$O + N_2 \rightarrow NO + N. \qquad (22)$$

The rate for (-20) has been given by Bortner[41] as

$$k_{-20} = 1.1 \times 10^{18}\ T^{-1.2}\ cm^6\ mole^{-2}\ sec^{-1}.$$

The rate for reaction (22) was measured by Glick, Klein, and Squire,[42] with the result subsequently modified by Duff and Davidson[43] to yield

$$k_{22} = 7 \times 10^{13} \exp(-75{,}000/RT)\ cm^3\ mole^{-1}\ sec^{-1}.$$

These rates were also converted to pseudo-reaction times, assuming a mixture of 2% O_2 and 2% O in N_2; the results are presented in Figure 6. Since reaction (-20) is termolecular, the normalized recombination time retains a pressure dependence. Here we take p = 4 atm, which is representative of the shock tube conditions for temperatures from 1000 to 1500°K. The exchange reaction (22) is slow and can be neglected. However, the recombination time for oxygen atoms becomes comparable to the vibrational-relaxation time for N_2 - O_2 mixtures for temperatures below approximately 1400°K. This will provide the lower limit on the temperature range of the N_2-O experiments.

It should be noted that the rate for oxygen atom recombination with N_2 as a catalyst (k_{-20}) is not well established, and a more realistic lower temperature limit for these experiments can be established by a direct measurement of oxygen atoms in the shock-heated gas. We have considerable experience in measuring O atom concentrations, both by chemiluminescence [44,45] and by resonance scattering [46,47], and we will attempt to apply these methods to the shock tube experiments.

The molecular oxygen produced by reactions (18) and (19) constitutes an additional species that can contribute to the vibrational relaxation of N_2. The relaxation of O_2 is considerably more rapid than that of N_2, as indicated on Figure 6, and the $O_2(v = 1)$ thus produced subsequently transfers energy to the N_2 by vibration-vibration exchange. Vibrational relaxation of N_2-O_2 mixtures has been studied, [8,40,48] and the transition probabilities required to account for the O_2 in these experiments are summarized in Figure 7. In the present program, therefore, only a limited number of tests on a single N_2-O_2-CO mixture have been performed to substantiate agreement with existing measurements.

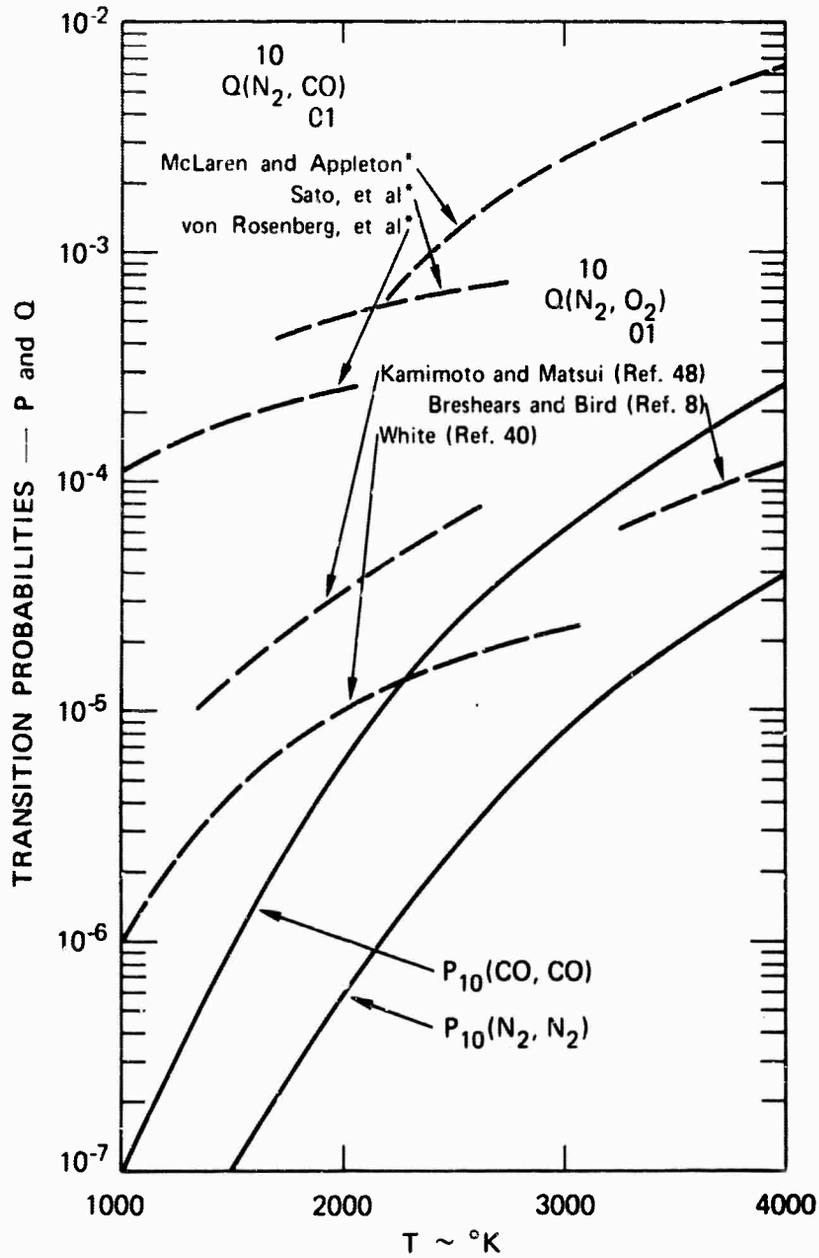

*Data summarized by McLaren and Appleton in Reference 53.

TA-8626-9

FIGURE 7 TRANSLATION-VIBRATION AND VIBRATION-VIBRATION TRANSITION PROBABILITIES FOR N_2, CO, AND O_2

In addition to the vibrationally-excited O_2 produced by normal collision processes behind the shock wave, the O_2 formed from $O + O_3$ [reaction (19)] may be highly vibrationally excited. McGrath and Norrish[49] flash photolyzed ozone and subsequently observed O_2 in the 12th to 17th vibrational levels, which they assumed was formed by way of reaction (19). However, Basco and Norrish[50] pointed out that the O formed in the photolysis of O_3 is $O(^1D)$ while that produced by thermal dissociation of O_3 is $O(^3P)$, and it is not known whether the reaction of $O(^3P)$ with O_3 also produces vibrationally-excited O_2. Since N_2 may be vibrationally excited by O_2(vib) through V-V processes as well as by $O(^3P)$ T-V reactions in this experiment, the uncertainty in the amount of O_2(vib) produced by Reaction (19) will cause an uncertainty in the rate of the N_2 - $O(^3P)$ process. This uncertainty will become larger at lower temperatures where Reaction (19) becomes increasingly faster than Reaction (18); its magnitude will be assessed during the data analysis.

From the above comparisons of chemical-reaction and vibrational-relaxation rates, we conclude that the thermal dissociation of ozone provides a satisfactory source of $O(^3P)$ atoms for the study of the vibrational relaxation of N_2 by $O(^3P)$ for temperatures above approximately 1400°K, providing that the contribution to the relaxation from O_2 formed in the dissociation process is adequately taken into account.

IR-Tracer Method

Millikan and White showed that the IR-tracer technique provided a satisfactory way of measuring the vibrational relaxation of shock-heated N_2 for temperatures down to approximately 1500°K. Here we describe the basis for the method in some detail. In this method, a small amount of CO is added to the N_2 test gas. Because N_2 and CO have similar vibrational energy levels (2331 cm^{-1} for N_2 and 2143 cm^{-1} for CO), the vibration-vibration (V-V) exchange between them is nearly resonant and therefore quite rapid. Pertinent measurements have been made by Sato[51], von Rosenberg, et al[52], and McLaren and Appleton;[53] a summary of transition probabilities for V-V exchange measured by these different workers, as summarized by McLaren and Appleton[53] is reproduced in Figure 7. It is noted that V-V transition probabilities $Q(\overset{10}{N_2},\underset{01}{CO})$ range from 10^{-4} at 1000°K to 10^{-2} at 4000°K. For comparison, translation-vibration (T-V) transition probabilities $P_{10}(N_2, N_2)$ for N_2-N_2 and $P_{10}(CO,CO)$, for CO-CO collisions based on vibrational relaxation data are also shown in Figure 7. P_{10} and the vibrational-relaxation time τ are related by

$$P_{10} = \frac{1}{\tau Z[1 - \exp(-h\nu/kT)]} , \qquad (23)$$

where Z is the collision frequency. From the correlations of Millikan and White[27], the T-V transition probabilities for N_2 by CO and for CO by N_2 are estimated to be essentially the same as those for N_2 by N_2 and for CO

by CO, respectively. It is seen that the V-V probabilities are two to three orders of magnitude greater than T-V probabilities across the entire temperature range. In view of the small fraction of CO present, it therefore is reasonable to assume that CO is in vibrational equilibrium with the N_2.

Decius[54] has shown that the fundamental-band radiation from an infrared-active molecule is proportional to the vibrational energy. Assuming a harmonic-oscillator model, the optical transition probabilities $A_{v,v-1}$ for $\Delta v = 1$ transitions from any vibrational level v are related to A_{10} by

$$A_{v,v-1} = vA_{10}. \tag{24}$$

Then the total radiation from fundamental-band transitions ($\Delta v = 1$) is

$$I = A_{10}h\nu \sum_{v=0}^{\infty} vn_v \equiv A_{10} \cdot E_V , \tag{25}$$

where n_v is the population of molecules in the vth level and E_V is the vibrational energy per unit volume. Now τ is given by the Landau-Teller formula as

$$\frac{dE}{dt} = \frac{\bar{E}(T) - E}{\tau} , \tag{26}$$

where $\bar{E}(T)$ is the vibrational energy that the gas would have if it were in equilibrium with the translational temperature. If the translational temperature is essentially constant during the relaxation process, as is the case for shock-heated N_2, equations (25) and (26) can be combined to yield

$$\frac{dI}{dt} = \frac{I_{max} - I}{\tau} , \tag{27}$$

where I_{max} is the asymptotic value. Thus the relaxation time can be determined from the slope of a semilogarithmic plot of $1 - (I/I_{max})$ versus time.

In practice, the infrared radiation monitored in these experiments does not encompass the entire fundamental band system as is required to ensure the equality of the second and third terms of equation (25). Rather, the spectral bandpass is limited to a more or less narrow interval by means of a filter or monochromator. Because the translational and rotational temperatures are essentially constant, however, the radiation from a portion of the band tends to be proportional to the total. In the present experiments, two filters with bandwidths differing by a factor of 4 give the same results for N_2 vibrational-relaxation times. As further verification of the validity of the IR-tracer method, Appleton[55] and Hanson and Baganoff[56] have obtained results by ultraviolet-absorption and endwall pressure measurements, respectively, that agree very well with the narrow-bandpass filter IR results of Millikan and White[36].

Experimental Arrangement

The 2-inch-diameter shock tube is made of stainless steel and has a 4.4-meter driven section. The test station is 33 cm from the end wall and is fitted with 4 window ports at 90° circumferential intervals. For the laser-schlieren tests, laser-quality antireflection coated quartz windows were fitted flush with the shock tube wall at the window centerline. Because of the cylindrical wall, there are 0.062-inch recessions at the edges of the 0.5-inch-diameter apertures. For IR tests, a recessed sapphire window (1-inch diameter, 0.375 in thick) is used; the other windows are Lucite blanks chosen to reduce IR reflections.

The shock tube was evacuated to a pressure of less than 10^{-6} torr before each test. The leak rate was approximately 5×10^{-5} Torr/minute, and the shot was fired within 3 minutes of closing the diffusion pump. The mechanical forepumps and the diffusion pump were cold trapped to -40°C by Freon refrigerator units to prevent backstreaming. The 99% N_2-1% CO, 95% N_2-5% CO, and 94% N_2-5% O_2-1% CO gas mixtures were obtained in premixed form from Matheson and have stated purities of 99.995%. (Mixtures containing O_3 will be formed by adding O_3 to the N_2-CO mixture.) The test gas was passed through a dry ice-acetone cold trap before entering the shock tube. Filling pressures ranged from 2 to 300 Torr. Cold hydrogen was used as the driver gas.

The laser-schlieren tests were carried out using a Spectra Physics Model 122 He-Ne laser, which has a near-field beam diameter of 0.7 mm and a divergence angle of 1.6 milliradians. The photodetector was a UDT Model No. PIN-81C which has a response time of 10 nsec and a response of 0.5 $\mu A/\mu W$. The nonamplified output of the photodiode was fed directly into a Tektronix 555 oscilloscope. A 7-meter optical path was achieved using two pentaprisms to fold the beam. Tests with the beam bypassing the test section showed that there were no vibration or acoustic effects.

For the IR tests, emission from a 2-mm-long volume element at the center of the shock tube was focused on a Philco-Ford Model ISC-363 indium antimonide photo-voltaic detector by means of an f/1, 2 in.-diameter IRTRAN II lens. The time response of the detector-amplifier system was checked by viewing the 4.1-micron radiation from CO_2 shocked to conditions where the vibrational relaxation is virtually instantaneous, and was found to be approximately 2.5 μsec. For tests of the N_2-CO mixtures, an OCLI filter centered at 4.65 microns with a 0.30-micron bandwidth was used; for the tests with the N_2-O_2-CO mixture, a 0.07-micron bandpass filter centered at 4.74 microns was used.

Results and Discussion

Laser-Schlieren Measurements

The measurements of the vibrational relaxation of N_2 by $O(^3P)$ by Breshears and Bird[8] were made using the laser-schlieren technique, and it was attempted in this program to use the same technique to extend those measurements to lower temperatures. In the laser-schlieren technique, the refraction of the laser beam by index-of-refraction gradients in the test medium is sensed by a photodetector (see Kiefer and Lutz[57] for a full discussion of the method). If the test medium is of width W and the moment arm from the test section to the detector is of length L, then the lateral displacement Δ of the beam at the detector is

$$\Delta = LW\frac{dn}{dy} , \qquad (28)$$

where dn/dy is the index-of-refraction gradient perpendicular to the laser beam. In applying this method to measurement of the vibrational relaxation of shock heated gases, we find that the "test medium" consists of three regions, namely, the core of the test gas, the wall boundary layers, and the windows. In the core of the gas, the index gradient is determined by a density gradient that results from the vibrational-relaxation process. In the boundary layers, turbulent eddies can also produce significant random density gradients. Finally stress waves in the windows induced by the large pressure rise across the shock wave cause index-of-refraction gradients. The success of the

laser-schlieren method depends on the predominance of the first effect over the last two. This is the case for N_2 at high temperatures where the vibrational energy content is fairly large and the relaxation time short so that the density gradient is reasonably large; furthermore, the boundary layer is laminar, at least over the relaxation region. These are the conditions under which Breshears and Bird[8] made their measurements. As temperature decreases, however, the density gradient rapidly decreases in magnitude, and the relaxation region begins to extend into the turbulent boundary layer zone. A typical laser-schlieren trace under these conditions is shown in Figure 8, where a noise signal is seen to dominate over the relaxation signal after about 10 microseconds. Because of an apparent periodicity of the noise observed in many tests, we suspected that it could arise from stress waves in the window, and some effort was devoted to the design of windows that might reduce this problem. However, experimental results that remove the windows as a primary noise source are presented in Figure 9. In this experiment, the inner surface of one window was mirrored. Trace A was obtained with the laser beam passing through the window and immediately reflected back onto the detector so that no gas effects were present. In trace B, the beam passed through the opposite window and across the shock tube, where it was reflected back through both media and onto the detector.

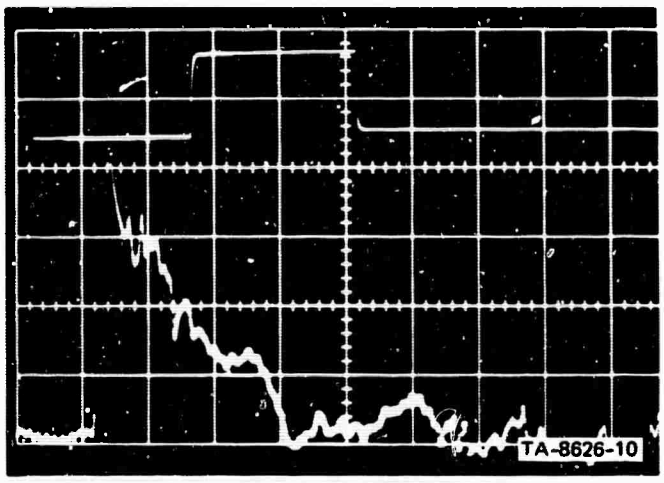

$M = 7.3$, $p_1 = 20$ TORR, $p_2 = 1400$ TORR, $T_2 \cong 3000^{\circ}$ K
UPPER TRACE: SHOCK SPEED MEASUREMENT
LOWER TRACE: LASER-SCHLIEREN SIGNAL, 5 μsec/cm

FIGURE 8 LASER-SCHLIEREN SIGNAL SHOWING DISTURBANCES DUE TO FLOW TURBULENCE

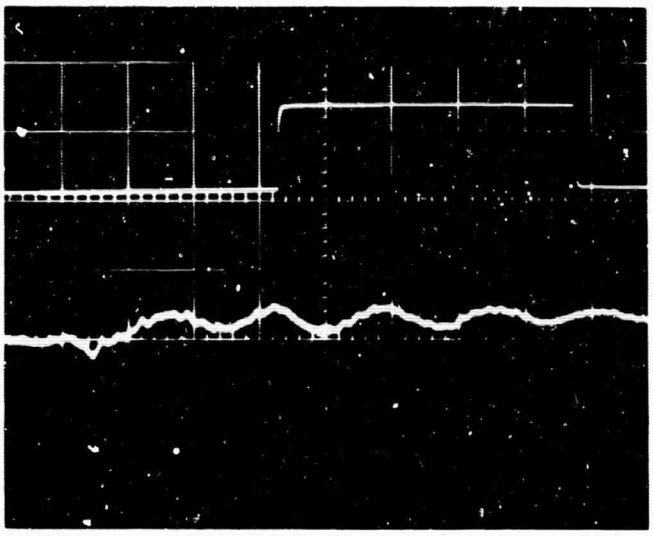

(a) LASER-SCHLIEREN SIGNAL DUE TO TWO PASSES THROUGH WINDOW. SENSITIVITY = 2 mV/cm, TIME SCALE = 10 μsec/cm.
M = 4.0, p_1 = 100 TORR, p_2 = 1800 TORR, T_2 = 1600° K

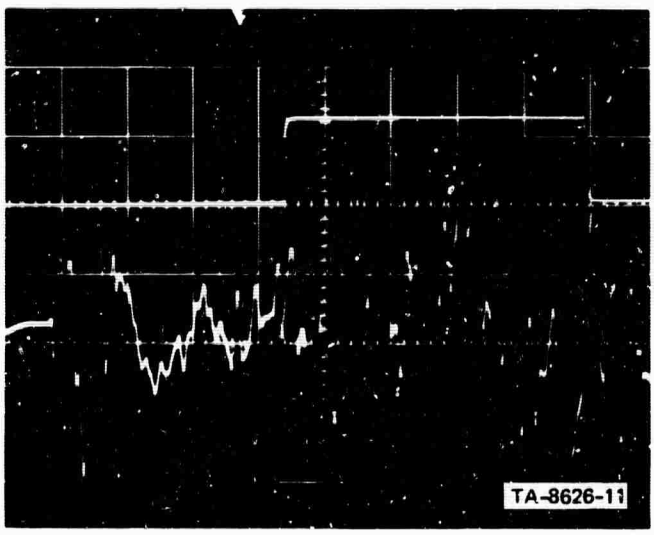

(b) LASER-SCHLIEREN SIGNAL DUE TO TWO PASSES THROUGH SHOCK-HEATED GAS PLUS WINDOW. SENSITIVITY = 10 mV/cm, TIME SCALE = 10 μsec/cm.

FIGURE 9 LASER-SCHLIEREN SIGNALS SHOWING RELATIVE CONTRIBUTIONS OF WINDOWS AND SHOCK-HEATED GAS

Whereas two passes through the window introduced only a lower frequency oscillation into the signal, two passes through the gas produced a very large noise. This shows rather conclusively that the disturbance is in the gas, and, in fact, must be in the turbulent boundary layers.

Two different approaches were tried in an attempt to eliminate the boundary-layer disturbances. In the first, small, thin windows were mounted in splitter plates, which were set 5 mm inside the shock tube walls on aerodynamically shaped hollow stems. In principle, the wall boundary layers will pass between the splitter plates and the walls, leaving a turbulence-free flow between the plates. The technique produced some reduction in the noise signal, but it was still inadequate for data analysis. In the second approach, regions of the shock tube walls 0.75 inch in radius upstream of the windows were made porous (15% geometric porosity), with plenum chambers behind the thin porous walls. When the shock wave passes, the differential pressure across the wall tends to "blow" the boundary layer through the wall, possibly leaving a turbulence-free flow between the windows. Again, this technique did not produce significant improvement in the intensity signal. It must be concluded that the laser-schlieren method is extremely sensitive to flow disturbances, and that the onset of any turbulence causes a fundamental limitation to the use of this technique.

Since other workers have experienced the same limitations with this method[58], it is not unique to any one shock tube facility.

In view of this limitation, we concluded that it is not possible to use the laser-schlieren method to study the vibrational relaxation of N_2 for temperatures much below 3000°K. Therefore, our efforts were shifted to the IR-tracer method which was described above.

IR-Tracer Measurements

To establish the proper performance of the shock tube, the IR detector system, and the data analysis techniques, we made a series of IR-tracer measurements of the vibrational relaxation of N_2 in a 99% N_2-1% CO mixture. Results covering the temperature range from 1300 to 3500°K are presented in the Landau-Teller plot of Figure 10, together with a curve representing the baseline results of Millikan and White[36]. Three values for each test are presented based on three methods of data evaluation. The value marked by a circular symbol is that relaxation time at which the intensity reaches 63.2% of asymptotic value. This is the value reported by Millikan and White. In addition, two results are reported that are based on different ways of evaluating the slopes of the semilogarithmic plot of $1 - I/I_{max}$ versus time. The first is a simple least-squares exponential fit to the data; the second is a non-linear (iterative) curve fit that chooses an optimum asymptotic value such that the least-squares deviations are minimized, i.e., the semi-

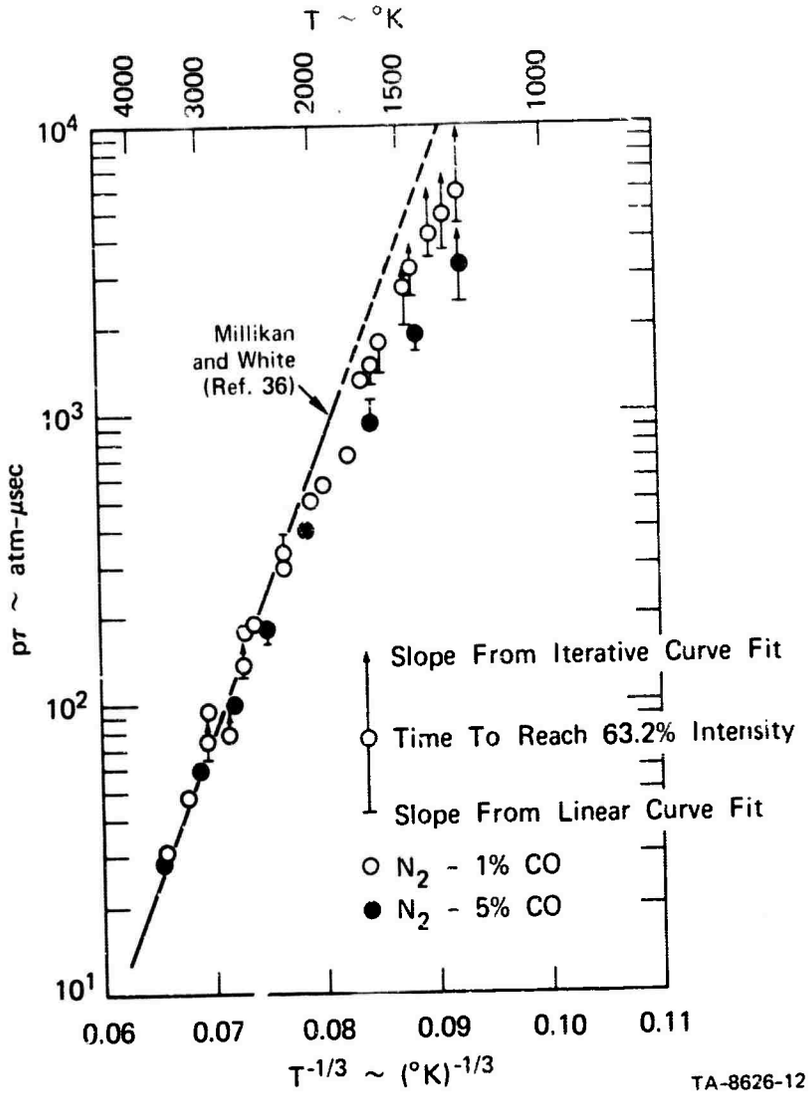

FIGURE 16 VIBRATIONAL RELAXATION TIMES FOR N_2 MEASURED BY IR-TRACER METHOD

logarithmic curves may be made more nearly linear by a new choice of the asymptote.

The high-temperature limit of the test results is due to the limited response time of the detector whereas in the low-temperature limit the vibrational-relaxation time of the N_2 exceeds the available test time in the shock tube, which is approximately 200 μsec. In the latter case, both boundary layer growth and shock speed attenuation tend to influence the IR asymptotic intensity, and therefore at the lower temperatures the iterative-curve-fit technique is expected to yield the most reliable values.

The present results agree very well with the earlier results of Millikan and White in the temperature range where they overlap. However, at lower temperatures there is a definite deviation from a straight-line extrapolation of those results, which would not be anticipated on the basis of existing theories[59,60] and which is larger than the experimental uncertainty. Similar deviations from a straight-line extrapolation have been observed for N_2 using the IR tracer method in another laboratory[61]. Also, Miller and Millikan[62] have recently reported low-temperature (200 to 400°K) deviations from extrapolated high-temperature results for CO-He and CO-H_2 systems, which they attribute to the influence of the attractive part of the potential at

these lower kinetic energies. However, this effect would not be expected to influence the present results at temperatures above 1000°K.

Although considerable effort has been expended in these experiments to minimize the presence of impurities, we must consider the possibility that the deviation of the results from a straight line is an impurity effect. In particular, species such as He, H_2O, and H_2 are known to have pronounced effects on vibrational relaxation data (c.f., Hooker and Millikan[63]). If we take a characteristic relaxation time of 10^{-6} atm-sec for N_2-impurity collisions (e.g., H_2) at T = 1000°K,[62] then an impurity level of about 50 ppm is sufficient to account for a reduction of the observed N_2 relaxation time by a factor of 2 below the "pure" gas value given by the extrapolated Millikan and White results. The specified impurity level of the Matheson test gas is less than 50 ppm total, which might typically include 5 ppm each of H_2, H_2O, and He. The use of H_2 as the driver gas raises the possibility of residual H_2 in the test section. However, the shock tube was evacuated to at least 10^{-6} Torr before each shot, and filling pressures were above 100 Torr for the low-temperature tests. This would tend to eliminate residual gases as a significant source of impurities.

Another possible cause of the deviation that cannot be overlooked at the lower temperatures is the more rapid excitation of CO compared

with N_2 (see Figure 6). Because of the rapid V-V exchange between N_2 and CO, the relaxation time of the mixture is given approximately by

$$\frac{1}{\tau_{mix}} \cong \frac{\Psi_{N_2}}{\tau_{N_2-N_2}} + \frac{\Psi_{CO}}{\tau_{CO-CO}} , \qquad (29)$$

where Ψ_i is the mole fraction of the respective gas. Since the relaxation time of CO is about 1/20th that of N_2 at 1200°K, the relaxation time will be reduced by 20% for a 99% N_2-1% CO mixture. For a 95% N_2-5% CO mixture, the relaxation time is reduced by 100%, and indeed, results presented in Figure 10 for this gas mixture do show a shorter relaxation time for the lower temperatures.

We conclude that the vibrational-relaxation time for pure N_2 is given by the extrapolated Millikan-White results, at least for temperatures down to ~ 1000°K, and that deviations from this curve are due to the increasingly important effects of even small concentrations of impurities and of the CO tracer. Nevertheless, the "deviated" results must be taken as the baseline for nominally pure N_2 when considering the effects of other species such as O_2 or O on the vibrational-relaxation time.

In the second phase of the measurements, the effect of O_2 was studied in a 94% N_2-5% O_2-1% CO mixture. In the first series of these tests, the intensity history showed a behavior illustrated by the oscilloscope traces of Figure 11, that is, instead of rising exponentially

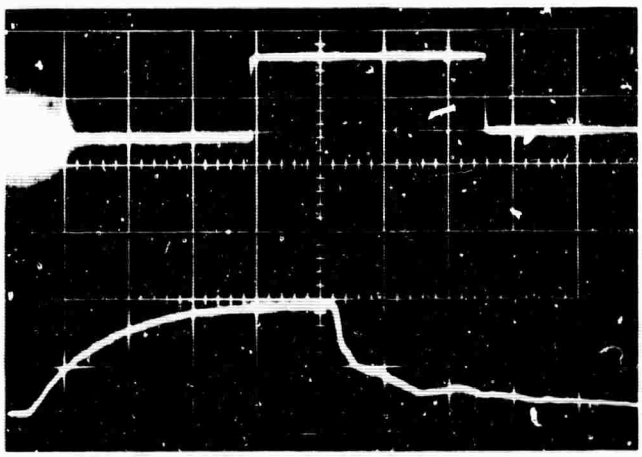

(a) INFRARED SIGNAL FROM N_2 - 1% CO.
SENSITIVITY = 100 mV/cm, TIME SCALE = 50 μsec/cm

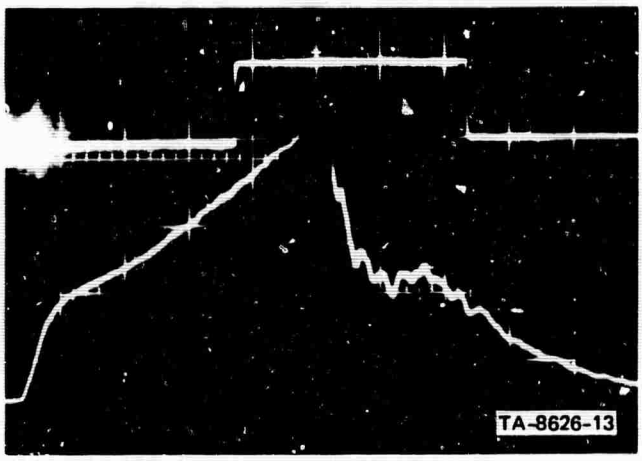

(b) INFRARED SIGNAL FROM N_2 - 5% O_2 - 1% CO.
SENSITIVITY AND TIME SCALE SAME AS FOR TRACE A.
M = 4.9, p_1 = 180 TORR, p_2 = 5000 TORR, T_2 1700° K

FIGURE 11 INFRARED EMISSION FROM SHOCK-HEATED N_2-CO AND N_2-O_2-CO MIXTURES SHOWING EXTRANEOUS RADIATION FROM N_2-O_2-CO MIXTURE

to an asymptotic value as is the case for N_2-CO mixtures (Trace A), the intensity broke away from the exponential and increased almost linearly for the duration of the available test time (Trace B). The filter in these tests was rather wide band, covering the spectral range from 4.49 to 4.80 microns, and it was felt that the extraneous radiation was from the 4.3-micron band of vibrationally excited CO_2, which had been formed from the CO and O_2. Therefore, a narrow-band filter in the ranges 4.71 to 4.78 microns was used. This new filter gave satisfactory results for temperatures up to approximately 2000°K, although the extraneous radiation reappeared at higher temperatures.

Results covering the range 1200 to 2000°K are presented in Figure 12, together with curves representing the N_2-only case. White[40] made similar measurements on five different N_2-O_2 mixtures using both CO tracer and interferometer techniques, and the curve presented in Figure 12 is based on his correlation of the results for all five mixtures. The present data agree with that correlation very well, much better, in fact, than did White's own data for a mixture containing 5% O_2. Thus we conclude that the present measurements are producing reasonable results, and that the V-V transition probabilities for N_2-O_2 collisions deduced by White[40] and others and presented in Figure 7 can be used with confidence.

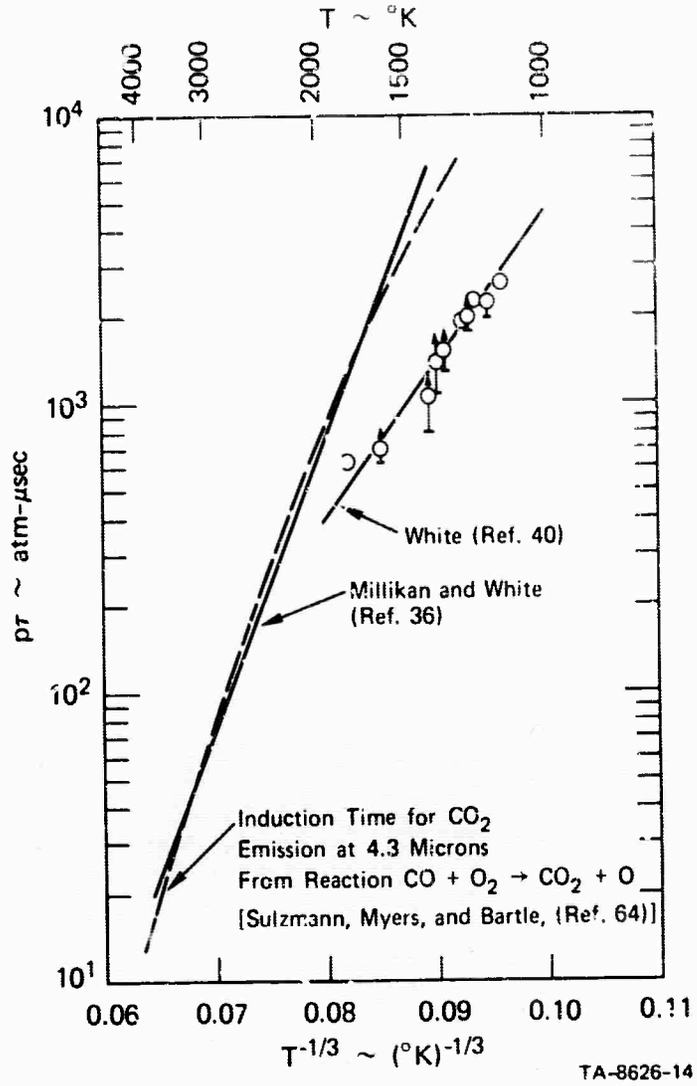

FIGURE 12 VIBRATIONAL RELAXATION TIMES FOR 94 PERCENT N_2-5 PERCENT O_2-1 PERCENT CO MIXTURES BY THE IR-TRACER METHOD

It is interesting to note that neither White nor Kamimoto and Matsui[48], who also made measurements in N_2-O_2 mixtures using the CO tracer technique, report problems of extraneous radiation as noted here, although those sets of measurements were also confined to temperatures below 2000 and 2650°K, respectively. The earlier noted speculation that the radiation is from CO_2 is appealing, particularly in view of the work of Sulzmann, Myers, and Bartle,[64,65] who studied the oxidation of CO in CO-O_2-Ar mixtures. In their study they simultaneously measured CO and CO_2 radiation at 5.07 and 4.25 microns, respectively, and found considerable CO_2 emission produced before completion of the CO vibrational relaxation. They also observed extraneous radiation at 5.07 microns, similar to that observed in the present study, which they attribute to CO_2 radiation in the long-wavelength wing of the 4.3-micron band. The primary reaction of interest is

$$CO + O_2 \rightarrow CO_2 + O. \tag{30}$$

These authors determined a rate constant for this reaction. In addition, however, they measured a characteristic time for the onset of 4.3-micron radiation from CO_2, which they express in the form

$$P\tau_{onset} = f(T)\,(\Psi_{CO} \cdot \Psi_{O_2})^{\frac{1}{2}} . \tag{31}$$

Using their values of f(T) and values of Ψ_{CO} and Ψ_{O_2} for the present

work, we calculated the radiation-onset time which is presented in Figure 12. This time is coincidentally nearly identical with the vibrational-relaxation time for pure N_2 and indicates that anomalous behavior might be expected for a 5% O_2 mixture at temperatures above 2000°K.

In the present study, however, we believe that all the radiation observed at 4.74 microns is from CO itself, rather than from CO_2, for two reasons. First, a series of tests made using a CO_2 filter centered at 4.07 microns with a 0.22-micron bandpass showed no significant CO_2 radiation for conditions where the 4.74-micron filter indicated a large extraneous signal. Secondly, in a limited number of tests, a 7-cm gas cell filled with either CO_2 or CO was placed between the shock tube and the IR detector. The CO_2 cell caused no change in the signal, but the CO cell eliminated almost all the anticipated and extraneous signals. On the other hand, if the extraneous radiation is from CO, it is surprising that the bandwidth of the filter should alter the results.

In view of these uncertainties, we can only state that a source of extraneous radiation of unknown origin emanating from mixtures containing CO and O_2 interferes with the desired signal from CO in the vicinity of 4.7 microns and therefore limits the usefulness of the IR-tracer technique to temperatures below 2000°K for mixtures of N_2-5% O_2-1% CO. In the temperature range of most importance for this program,

below 2000°K, this radiation will provide no problem. Furthermore, experience in other laboratories with different ratios of the same gases indicates that the method may yield results at even higher temperatures for the N_2-O_2-O-CO mixtures required in the remainder of this study.

Extension of the IR-Tracer Method to the N_2-O System

The next step in this program will be to conduct a series of IR measurements on mixtures containing 1 to 2% O_3 and 1% CO in N_2. The reaction between O_3 and CO is known to be very slow at room temperature,[66] and no significant decomposition of O_3 in the test gas by this mechanism is anticipated. After passage of the shock wave, the O_3 dissociates to form O and O_2, and reactions between CO and O or O_2 would be important. The primary reactions are

$$CO + O_2 \rightleftharpoons CO_2 + O \qquad (30)$$

and

$$CO + O + M \rightleftharpoons CO_2^* + M. \qquad (32)$$

In contrast to the onset time for CO_2 emission discussed above, Sulzmann, Myers, and Bartle[64] have deduced the rate for reaction (30) as

$$k_{30} = 3.5 \times 10^{12} \exp(-51{,}000/RT) \text{ cm}^3 \text{ mole}^{-1} \text{ sec}^{-1}.$$

Rates for reaction (32) have been reported for room temperature[67] and in the interval 2800 to 3600°K.[68] In addition, recent unpublished room temperature measurements have been made by Black and Slanger of this laboratory and by Stuhl and Niki of Ford Research Laboratory. These recent room temperature results and the higher temperature results are consistently represented by the expression

$$k_{32} = 8 \times 10^{13} \exp(-3{,}000/RT) \text{ cm}^6 \text{ mole}^{-2} \text{ sec}^{-1}.$$

Again, we can assess the importance of these reactions in the N_2-O vibrational-relaxation measurements by converting these rates to pseudo-reaction times. The calculations assume a mixture of 2% O_2, 2% O and 1% CO in N_2; for the termolecular reaction (32) a total pressure of 4 atm is used. The results are also presented in the earlier Figure 6 for comparison with the vibrational-relaxation times of the N_2 mixtures. We see that both of these reactions are negligibly slow, at least for temperatures above 1000°K.

The CO_2 formed in reaction (32) is in an electronically excited state, which is subsequently deactivated either radiatively or by collision. Myers and Bartle[69] showed that the radiation intensity is proportional to the product of CO and O concentrations, i.e.,

$$I = A(CO)(O). \tag{33}$$

Thus this chemiluminescent reaction offers a convenient method of monitoring the concentration of O atoms behind the shock wave.

Summary

An experimental program has been formulated to measure the vibrational relaxation of N_2 by O atoms by an IR-tracer method using small admixtures of CO. The shock tube facility and IR measurement instrumentation have been developed and checked, and a considerable number of measurements have been made on N_2-1% CO, N_2-5% CO, and N_2-5% O_2-1% CO mixtures. The vibrational-relaxation times for the N_2-CO mixtures show excellent agreement with existing measurements for temperatures above approximately 1800°K; for lower temperatures, the present results fall below a straight-line extrapolation of the higher temperature data. This deviation can be attributed to the effects of the additive CO and to possible impurity levels of less than 50 ppm of H_2, He, or H_2O.

The vibrational-relaxation times for the N_2-O_2-CO mixture also agree well with existing measurements for temperatures in the range 1200 to 1800°K. At higher temperatures, extraneous IR radiation obscures the expected signal. This extraneous radiation can be attributed to the CO, but its cause has not been identified.

An examination of existing rate measurements shows that the addition of CO to N_2-O_2-O mixtures should not introduce any limitations in these measurements. Rather, a low-temperature limit of approximately

$1400^{o}K$ is imposed by the recombination of O atoms with an N_2 catalyst. No fundamental high-temperature limit is anticipated, although such a conclusion must be stated cautiously in view of the yet-unexplained problem experienced in the N_2-O_2-CO tests.

REFERENCES

1. J.C.G. Walker, Planet. Space Sci. 16, 321 (1968).
2. L. F. Phillips and H. I. Schiff, J. Chem. Phys. 36, 3283 (1962).
3. J. E. Morgan, L. F. Phillips, and H. I. Schiff, Discussions Faraday Soc. 33, 118 (1962).
4. J. E. Morgan and H. I. Schiff, Can. J. Chem. 41, 903 (1963).
5. K. L. Wray, E. Feldman, and P. Lewis, J. Chem. Phys. 53, 4131 (1970).
6. R. E. Murphy, J. W. Rogers, and M. H. Bruce, "Energy Partition in the $N + NO \rightarrow N_2 \nleftarrow + O$ Reaction," presented at the DASA High Altitude Nuclear Effects Symposium at Stanford Research Institute, August 1971
7. E. R. Fisher and E. Bauer, private communication, 1971.
8. W. D. Breshears and P. F. Bird, J. Chem. Phys. 48, 4768 (1968).
9. R. A. Young, G. Black and T. G. Slanger, J. Chem. Phys. 49, 4758 (1968).
10. H. Hamazaki and R. J. Cvetanović, J. Chem. Phys. 40, 582 (1964).
11. K. F. Preston and R. J. Cvetanović, J. Chem. Phys. 45, 2888 (1966).
12. G. Paraskevopoulos and R. J. Cvetanović, J. Amer. Chem. Soc. 91 7572 (1969).
13. N. P. Carleton, F. J. LeBlanc, and O. Oldenberg, Bull. Am. Phys. Soc. 11, 503 (1966); J. Chem. Phys. 45, 2200 (1966).

14. D. R. Snelling and E. J. Bair, J. Chem. Phys. 47, 228 (1967); 48, 5737 (1968).

15. J. F. Noxon, J. Chem. Phys. 52, 1852 (1970).

16. W. B. DeMore, J. Chem. Phys. 52, 4309 (1970).

17. M. Loewenstein, J. Chem. Phys. 54, 2282 (1971).

18. L. Wallace and M. B. McElroy, Planet. Space Sci. 14, 677 (1966).

19. J. D. Lambert, Atomic and Molecular Processes, Ed. by D. R. Bates, (Academic Press, New York, 1962), p. 783.

20. A. Dalgarno, Planet. Space Sci. 10, 19 (1963).

21. C. C. Rankin and J. C. Light, J. Chem. Phys. 46, 1305 (1967).

22. A. L. Schmeltekopf, F. C. Fehsenfeld, G. I. Gilman, and E. E. Ferguson, Planet. Space Sci. 15, 401 (1967).

23. D. Rapp and P. Englander-Golden, J. Chem. Phys. 40, 573 (1964); 40, 3120 (1964).

24. D. Rapp, J. Chem. Phys. 43, 316 (1965).

25. R. A. Young, G. Black, and T. G. Slanger, J. Chem. Phys. 48, 2067 (1968).

26. R. A. Young, G. Black, and T. G. Slanger, J. Chem. Phys. 50, 303 (1969).

27. R. C. Millikan and D. R. White, J. Chem. Phys. 39, 3209 (1963).

28. Y. Beers, Introduction to the Theory of Error (Addison-Wesley Publishing Company, Inc., Cambridge, Massachusetts 1953), p. 23.

29. "Excitation and Dexcitation of Vibration in N_2 by Oxygen Atoms," Semiannual Technical Report No. 1 on Contract No. DAHC04-70-C-0036, by G. Black, D. C. Lorents, and D. J. Eckstrom, December 1970.

30. J. H. Kiefer and R. W. Lutz, 11th Symposium Comb., Berkeley, California, 67 (1967) and subsequent comments by J. G. Parker and S. W. Benson.

31. C. W. von Rosenberg, Jr., R. L. Taylor and J. D. Teare, J. Chem. Phys. 54, 1974 (1971).

32. C. W. von Rosenberg, Jr. and K. L. Wray, AVCO Everett Research Report 345, December 1970.

33. S. H. Bauer and S. C. Tsang, Phys. Fluids 6, 182 (1963).

34. E. Bauer, E. R. Fisher, and F. Gilmore, J. Chem. Phys. 51, 4173 (1969).

35. E. Bauer, private conversation.

36. R. C. Millikan and D. R. White, J. Chem. Phys. 39, 98 (1963).

37. W. M. Jones and N. Davidson, J. Amer. Chem. Soc. 84, 2868 (1962).

38. B. F. Myers and E. R. Bartle, J. Chem. Phys. 48, 3935 (1968).

39. K. L. Wray, J. Chem. Phys. 38, 1518 (1963).

40. D. R. White, J. Chem. Phys. 49, 5472 (1968).

41. M. H. Bortner, National Bureau of Standards Technical Note 484, May 1969.

42. H. S. Glick, J. J. Klein, and W. Squire, J. Chem. Phys. 27, 850 (1957).

43. R. E. Duff and N. Davidson, J. Chem. Phys. 31, 1018 (1959).

44. R. A. Young and G. Black, J. Chem. Phys. 44, 3741 (1966).

45. R. A. Young and G. Black, Planet. Space Sci. 14, 113 (1966).

46. T. G. Slanger and G. Black, J. Chem. Phys. 53, 3717 (1970).

47. T. G. Slanger and G. Black, J. Chem. Phys. 53, 3722 (1970).

48. G. Kamimoto and H. Matsui, AIAA J. 7, 2358 (1969).

49. W. D. McGrath and R.G.W. Norrish, Proc. Roy. Soc. (London) A242, 265 (1957).

50. N. Basco and R.G.W. Norrish, Discussions Faraday Soc. 33, 99 (1962).

51. Y. Sato, S. Tsuchiya, and K. Kuratani, J. Chem. Phys. 50, 1911 (1969).

52. C. W. von Rosenberg, K.N.C. Bray, and N. H. Pratt, to be published.

53. T. I. McLaren and J. P. Appleton, M.I.T. Fluid Mechanics Laboratory Publication No. 70-10, November 1970.

54. J. C. Decius, J. Chem.Phys. 32, 1262 (1960).

55. J. P. Appleton, J. Chem. Phys. 47, 3231 (1967).

56. R. K. Hanson and D. Baganoff, J. Chem. Phys. 53, 4401 (1970).

57. J. H. Kiefer and R. W. Lutz, J. Chem. Phys. 44, 658 (1966).

58. W. D. Breshears, private communication.

59. L. Landau and E. Teller, Physik. Z. Sowjetunion 10, 34 (1936).

60. R. N. Schwartz, Z. I. Slawsky, and K. F. Herzfeld, J. Chem. Phys. 20, 1591 (1952).

61. D. J. Seery, United Aircraft Research Laboratory, private communication.

62. D. J. Miller and R. C. Millikan, J. Chem. Phys. 53, 3384 (1970).

63. W. J. Hooker and R. C. Millikan, J. Chem. Phys. 38, 214 (1963).

64. K.G.P. Sulzman, B. F. Myers, and E. R. Bartle, J. Chem. Phys. 42, 3969 (1965).

65. B. F. Myers, K.G.P. Sulzmann, and E. R. Bartle, J. Chem. Phys. 43, 1220 (1965).

66. K. Schofield, Planet. Space Sci. 15, 643 (1967).

67. V. N. Kondrat'ev and I. I. Ptichkin, Kinetika i Kateliz 2, 492 (1961).

68. T. A. Brabbs and F. E. Belles, 11th International Symposium on Combustion, University of California, Berkeley, 1966.

69. B. F. Myers and E. R. Bartle, J. Chem. Phys. 47, 1783 (1967).